Desalination and Water Treatment
www.deswater.com
doi: 10.5004/dwt.2020.24726

175 (2020) 115–124
January

Removal of chlornitrofen pollutants from water by modified humic acid-based hydrophobic adsorbent

Shilin Zhao[a,c,*], Feng Luo[c], Yueyue Shen[a,b,*], Fang Shen[c], Yang Tang[c], Dairui Xie[c], Saeed Rehman[b], Meng Jiang[c], Yamei Jiang[c]

[a]*Key Laboratory of Land Resources Evaluation and Monitoring in Southwest, Ministry of Education, Sichuan Normal University, Chengdu, Sichuan 610066, China, Tel./Fax: +86 02884761393; emails: zhaoslin@aliyun.com (S.L. Zhao), yshen028@126.com (Y.Y. Shen)*
[b]*School of Environment and Energy, South China University of Technology, Guangzhou 510006, China, email: Saeed_Rehman89@yahoo.com*
[c]*College of Chemistry and Materials Science, Sichuan Normal University, Chengdu, Sichuan 610068, China, emails: 302581116@qq.com (F. Luo), 1286749385@qq.com (F. Shen), 1837420762@qq.com (Y. Tang), 2416901113@qq.com (D.R. Xie), 1373592674@qq.com (M. Jiang), 1065067145@qq.com (Y.M. Jiang)*

Received 14 February 2019; Accepted 26 July 2019

ABSTRACT

Humic acid (HA) is considered as a ubiquitous natural resource around the globe and a common pollutant in the aqueous environment. In this case, HA was modified via simple etherification reaction and a new hydrophobic adsorbent (HAEE) was synthesized for removal of chlornitrofen pollutants (COPs) from aqueous solutions. The adsorption behaviors of HAEE toward COPs, including chlornitrofen (CNP), 2,4,6-trichlorophenol (2,4,6-TCP) and p-nitrophenol (PNP) from aqueous solutions were investigated. As a result, the HAEE adsorbent exhibited excellent adsorption performances for both single pollutant and multi-component COPs (removal efficiency > 95%). Meanwhile, the negligible pH influence (pH 4~8), short equilibrium time (8 h) and satisfactory reusability were also observed. Desorbed pollutants were completely degraded by a fluorine-based titanium dioxide-based photocatalyst under visible-light irradiation for the innocuous treatment. Furthermore, it is revealed that the hydrophobic interaction is a dominant force during adsorption process. These results suggest that hydrophobic HAEE adsorbent is expected to be a promising option for the treatment of various COPs in water/soil environment.

Keywords: Humic acid; Hydrophobicity; Adsorption; Chlornitrofen pollutants; Photocatalyst

1. Introduction

Chlornitrofen (CNP), a persistent organic pollutant, has been widely used during the 1970s and 1990s. It has been confirmed that not only chlornitrofen but also its degradation products namely 2,4,6-trichlorophenol (2,4,6-TCP) and p-nitrophenol (PNP) have poor water solubility with high toxicity, which are difficult to be decomposed in natural aqueous/soil environment and can easily accumulate in fatty tissues of organs, causing potential health threats [1–3]. Although the use of CNP with extreme toxicity has been banned in most of the countries for more than 20 years, CNP, 2,4,6-TCP and PNP are still detected in aqueous and soil environment [4,5]. Dreadfully, these residual chlornitrofen pollutants (COPs) inevitably generate a large amount of polluted soil sites due to their strong stability. Currently, the problem of highly COPs-polluted soil has becoming one of the most concerned issues. In addition, soil washing is one of the most efficient technologies for removing organic pollutions, including COPs, from polluted soil. Consequently, further issues emerged following the collected COPs-contained waste washing solution.

* Corresponding authors.

Adsorption is currently the efficient method for the purification of aqueous solutions with organic contaminations. Many efforts have been dedicated to developing adsorbents for organic pollutions in aqueous environment, including activated carbon for removing trichloroethene [6], γ-Al_2O_3 for adsorbing phenol [7] and reduced graphene oxide for removing naphthylamine [8], etc. Unfortunately, there are very little researches on the removal of high toxic COPs, especially about the development of adsorption materials for CNP and its degradation products in aqueous environment, such as washing solutions. Hence, the development of effective sorbents is urgent in order to solve COPs polluted issues.

Lipoid-type adsorbents may be preferable because of the hydrophobic nature of COPs. From this point of view, lipoid-type adsorbents are able to adsorb COPs through "like dissolves like" principle; moreover, these adsorbents can be recycled via organic solvent washing. Previous findings have shown that lipoid-type adsorbents exhibited great potential for effective removal of organic pollution from aqueous solution, for example, polyamide decorated triolein was used for adsorptive removal of nitrobenzene [9], triolein-embedded activated carbon showed a high adsorption capacity of dieldrin [10].

Humic acid (HA) is a ubiquitous natural resource with many functional groups, including carboxylic acid, alcohol, phenolic compounds, aldehydes, and methoxyl (Possible chemical structure of HA in Fig. 1). Thus, it makes sense to prepare novel functional materials using HA as raw material. On the other hand, HA will react with chlorine during water treatment and produce trihalomethanes, which is a potential carcinogen [11,12]. Hence, the HA-based adsorbent is of practical importance and interest.

Prior work has documented the potential performance of HA when used as the supporting matrix of adsorption material [13]: a lipoid-type adsorbent (HA-M), which was prepared by using HA immobilized monoolein via simple esterification, preserves high adsorption capacities to both chlorobenzene compounds and organochlorine pesticides. Based on these, it looks possible that HA-M can be further chemically grafted with various hydrophobic raw materials (such as glycerol triglycidyl ether) via etherification due to its abundant functional groups.

The work presented herein is to develop a new hydrophobic adsorbent for treatment of various COPs in water/soil environment. To evaluate the adsorptive removal properties of the prepared hydrophobic adsorbent to COPs, CNP, 2,4,6-TCP and PNP were utilized as the target contaminations in aqueous environment. The influence of pH on the adsorption capacity of COPs, the adsorption kinetics and the adsorption isotherms were systematically investigated. Furthermore, desorbed pollutants were completely degraded by a fluorine-based titanium dioxide-based photocatalyst under visible-light irradiation for the innocuous treatment. The hydrophobic adsorbent has exhibited satisfactory performance in treatment of COPs-contained aqueous solution.

2. Materials and experiments

2.1. Materials

Glycerol triglycidyl ether was obtained from Changshu Jiafa Chemical Ltd., China. Humic acid (HA; CAS: 1415-93-6) was purchased from Changshu Jiafa Chemical Co., Ltd. (China). Hexane was of analytical grade (ChengDu Kelong Chemical Co., Ltd., China). Chlornitrofen (CNP), 2,4,6-trichlorophenol (2,4,6-TCP) and p-nitrophenol (PNP) were purchased from Aladdin Industrial Corporation, (Shanghai, China).

HA-M was prepared according to the methods reported in our previous study [13]: in brief, monoolein (CAS: 111-03-05) was esterificated with HA using H_2SO_4 as catalyst. The resulting HA-M (1 g) was placed in a three-necked flask containing minute water. Then, the mixture was stirred at 333 K for 1 h while pH was adjusted to 5 by 0.2 mol/L NaOH. Glycerol triglycidyl ether (GTE; CAS: 13236-02-7; 25%wt of HA-M) was gently dropwise added, along with few drops of acetone. The etherification reaction was performed at 333 K

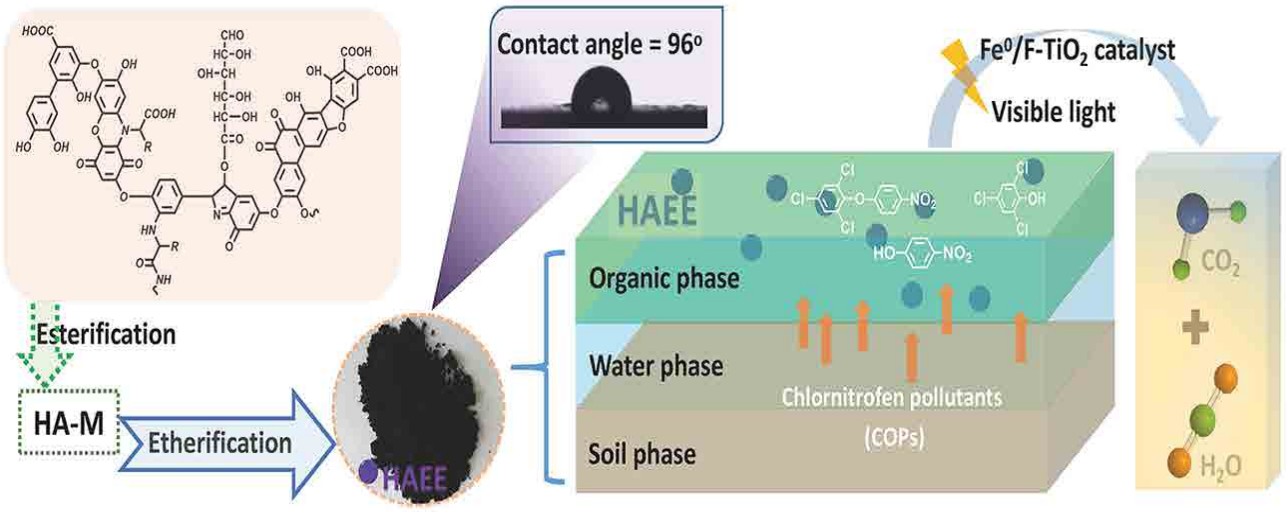

Fig. 1. Diagram of experiment procedure.

for 6 h with continued stirring. After the reaction, the mixture was cooled down to room temperature, following by centrifugation (4,000 r/min), and drying at 323 K. The obtained product was humic acid ester ether product (HAEE) and the preparation process can be illustrated by two major reaction steps which are shown as follows:

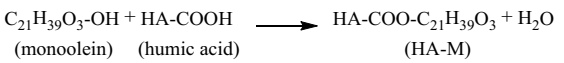

(1)

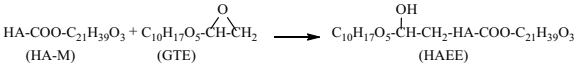

(2)

2.2. Experiments

Various COPs solutions used in this experiment were diluted by deionized water from the stock solutions. The adsorption system was kept sealed during all batch experiments.

2.2.1. pH influences on the adsorption capacity

0.02 g of HAEE was added into 50 mL of COPs solutions (10 mg/L of NCP; 10 mg/L of 2,4,6-TCP; 20 mg/L of PNP). The solution pH was adjusted in the range of 4–8 using HCl solutions (0.2 mol/L) and NaOH solutions (0.2 mol/L). The mixture solution was shaken at 293 K for 8 h to achieve the adsorption progress. When the adsorption was completed, the mixture solution was filtered. The collected filtrate was extracted by hexane for three times, then 0.2 g NaCl was added into the collected hexane solution to increase the ionic strength of organic matters. Subsequently, the collected organic phase was dehydrated using anhydrous sodium sulfate and precisely diluted to 10 mL via hexane. The obtained solutions were further filtered by passing through an organic membrane (0.45 μm), the concentrations of PNP was detected by ultraviolet spectrophotometer (Alpha-1900, Shanghai Puyuan Ltd., China; 398 nm) while the concentrations of NCP or 2,4,6-TCP in these filtrates were analyzed by gas chromatograph (GC, D7900, Teccomp Ltd., China). Besides, the organic membrane filter had no adsorption to COPs. Adsorption capacities of HAEE (q_e, mg/g) were calculated by Eq. (3):

$$q_e = \frac{(C_0 - C_t)V}{M} \tag{3}$$

where C_0 (mg/L) and C_t (mg/L) are the initial concentrations of COPs and the remaining concentration at time t, respectively, V (L) is the volume of aqueous solution and M (g) is the mass of adsorbent used.

2.2.2. Hydrophobicity influences on the adsorption capacity

In order to regulate and control the hydrophobicity of HAEE, different dose of glycerol triglycidyl ether (GTE) was added in the preparation process, respectively (15%wt, 25%wt, 50%wt, 100%wt and 200%wt of HA-M). With various hydrophobicity, the obtained HAEE (0.02 g) was added into 50 mL of solutions (10, 20, 30, 40, 50 mg/L of CNP, or 10, 20, 50, 100, 200 mg/L of 2,4,6-TCP, or 10, 20, 50, 100, 200 mg/L of PNP). The solution pH was adjusted to 7.0, while the adsorption process was conducted at 298 K with constant shaking for 8 h.

2.2.3. HAEE dose influences on the adsorption capacity

0.01, 0.02, 0.05, 0.10 or 0.20 g of HAEE was added into 50 mL of COPs solutions (50 mg/L of NCP, or 100 mg/L of 2,4,6-TCP, or 100 mg/L of PNP), respectively. Solution pH was adjusted to 7.0, while the adsorption process was conducted at 298 K with constant shaking for 8 h.

2.2.4. Adsorption kinetics

0.02 g of HAEE was added into 50 mL of solutions (30 mg/L of CNP, or 50 mg/L of 2,4,6-TCP, or 50 mg/L of PNP). The solution pH was adjusted to 7.0, while the adsorption process was conducted at 298 K with constant shaking, promising that lipophilic HAEE disperse well in the heterogeneous adsorption system formed by COPs and HAEE. The concentration of COPs in the organic phase was measured at different intervals, and the adsorption capacities at time t (min) were obtained by mass balance calculation, which were denoted as q_t (mg/g). The adsorption kinetic data were further fitted by the pseudo-first-order rate model, and the pseudo-second-order rate model, which are expressed as Eqs. (4) and (5):

$$\log(q_e - q_t) = \log q_e - \frac{k_1}{2.303}t \tag{4}$$

$$\frac{\mathrm{t}}{q_t} = \frac{1}{k_2 q_e^2} + \frac{t}{q_e} \tag{5}$$

where q_e (mg/g) and q_t (mg/g) are the adsorption amount of COPs at equilibrium and time t (h), respectively; k_1 (h^{-1}) and k_2 (g/(mg h)) are the rate constants.

2.2.5. Adsorption isotherms

Adsorption isothermal experiments were conducted with various initial concentrations of COPs. The solution pH was adjusted to 7.0 and the adsorption processes were carried out at 293, 208, 303 K for 8 h, respectively. The concentration of COPs in the extracted phase was measured by GC. The adsorption capacities at equilibrium (q_e) were obtained by mass balance calculation. Adsorption isotherms data were fitted by Freundlich equations.

2.2.6. Effect of coexisting organic pollutants

Benzene and phenol were utilized as coexisting organics to investigate the removal efficiency of HAEE adsorbent to COPs. Absorption experiments were carried out by adding 0.02 g of HAEE into 50 mL solutions of 2,4,6-TCP, respectively. The concentrations of each kind of organic pollutants were fixed at 0.5 or 1.0 g/L. Initial pH of the solutions was adjusted 7.0. Batch experiments were conducted at 298 K with constant shaking for 8 h. The concentrations of 1,3,5-TCB in the solutions were analyzed by GC.

2.3. Adsorption efficiency in multi-component aqueous solutions

0.02 g of HAEE was added into a series of 50 mL aqueous solutions, which contains CNP, 2,4,6-TCP and PNP with

different concentrations. The initial pH of the solutions was adjusted to 7.0 and the adsorption was carried out under constant stirring for 8 h. After adsorption, the remaining COPs concentrations were determined.

2.4. Regeneration of HAEE

Regeneration of HAEE was performed in desorbing solution of methylene chloride. 0.02 g of HAEE has been used to adsorb the 2,4,6-TCP (20 mg/L, 50 mL) and then was eluted in 20 mL methylene chloride with shaking at 298 K for 1 h. Finally, the HAEE was reused for the adsorption of 2,4,6-TCP.

2.5. Photocatalytic degradation and mineralization of COPs.

A simple and effective photocatalyst was developed for Fenton-like photocatalytic degradation and mineralization of 2,4,6-TCP eluted from HAEE. The catalyst was prepared as follows: 10 mL of titanium tetraisopropoxide was dissolved in 30 mL of absolute ethanol under constant stirring at 313 K. Subsequently, $Fe(NO_3)_3{\cdot}9H_2O$ was slowly added (mass ratio of Fe to Ti was 10%) and the mixture was stirred at 343 K for 30 min. Meanwhile, 10 mL of absolute ethanol was mixed with 5 mL water, followed by addition of HF (mass ratio of F to Ti was 0.05). Subsequently, this mixture was added into initial solution drop by drop with vigorous stirring, and then kept statically for 24 h. Afterwards, the gel was dried at 353 K for 24 h. The dried gel was reduced by $NaBH_4$ in nitrogen condition, and then calcined at 573 K for 6 h under vacuum. The obtained catalyst was entitled as $Fe^0/F\text{-}TiO_2$.

Photocatalytic experiments were carried out in a 100 mL photocatalytic reactor utilizing 0.05 g $Fe^0/F\text{-}TiO_2$. Metallic-additive lamp was used as the radiation source while UV light ($\lambda < 420$ nm) was filtered. Concentration of 2,4,6-TCP as well as chloride ion and total organic carbon of the 2,4,6-TCP solution was measured.

3. Result and discussion

3.1. Characterization

As shown in Fig. 2, hydroxyl groups had endowed HA with enough hydrophilicity. HA-M is dispersed in organic phase due to its enough hydrophobic property, though a few HA-M contained soils existed at interface between organic and water phases. Notably, the HAEE adsorbent just dispersed in organic phase after the modification with hydrophobic GTE. Additionally, the as-obtained HAEE could finely disperse well in organic/aqueous/soil heterogeneous system following constant shaking.

FT-IR spectra confirmed the existence of considerable hydrophobic groups in HAEE, such as –C=C, –COOH, –C–O– [14,15]. It was clear that this adsorbent had been successfully modified via etherification.

3.2. Single-component aqueous solutions

The adsorption performances of HAEE to three typical COPs were investigated. When solution pH was 7.0, the adsorption capacities of HAEE to all COPs were close to 23, 24 and 47 mg/g for CNP, TCP and PNP, respectively (Fig. 3a). Besides, there was only a negligible influence of pH on adsorption capacity, since the pH changes had least effect on the dominant adsorption mechanism (π–π interaction). Relatively high pHs and ionic strengths would promote the dissociation of hydroxyls in HA, then increase its chelating effect to various metal ions [16]. Obviously, hydrophobic COPs do not have an electron accepting ability. Additionally, the benzene rings in the HAEE can form "hydrophobic bond" with COPs. Hence, the adsorption process is dominated by the hydrophobic interactions between HAEE and COPs. This adsorbent is expected to have practical potential in a practical pH environment.

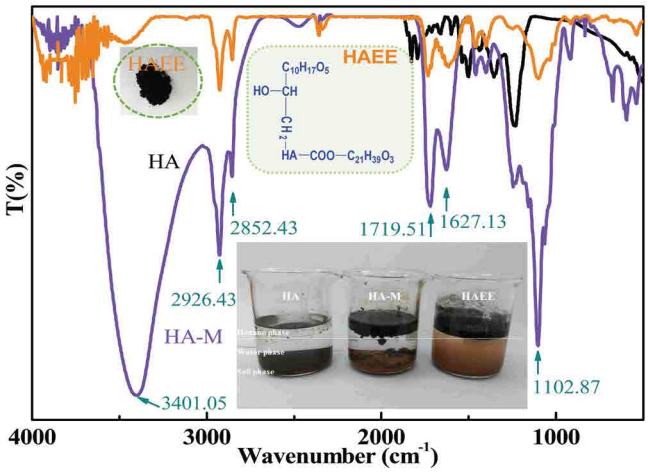

Fig. 2. FT-IR spectra and photograph of HA, HA-M and HAEE in hexane/water/soil system.

When the adsorbent dosage was at the maximum value (0.2 g), the adsorption capacities are 24.09, 37.80 and 23.08 mg/g for CNP, TCP and PNP, respectively. However, the amount of COPs adsorbed per unit mass of the adsorbent decreased considerably with increase of adsorbent dosage (Fig. 3b), which was mainly due to adsorption sites remaining unsaturated during the adsorption process [17]. The removal rates were more than 90% for both CNP and PNP. However, the adsorption removal rates of HA toward CNP were always less than 50% according to contrast test.

The overall effect of GTE dosage on CNP removal rate was studied in the first place, and the results are shown in Fig. 3c. Obviously, all the CNP removal rates were close to 90% no matter what the amount of GTE dosage was. The maximum CNP removal rate (96.58%) could be found when the GTE dosage was 25wt.% of HA-M, which was closest to the removal performance as the GTE dosage was 100wt.% of HA-M.

To further investigate the effect of GTE dosage on the adsorption removal performance toward all COPs, the two typical GTE dosages (25wt.% and 100wt.% of HA-M) were studied at different initial concentrations. The results are shown in Figs. 3d, 3e and 3f. A greater weight percentage (100wt.% of HA-M) always lead to higher adsorption capacities for each COPs as well as a greater contact angle (107°) between water and the HAEE surface (Fig. 4). It is easy to find the difference of the adsorption capacities among CNP,

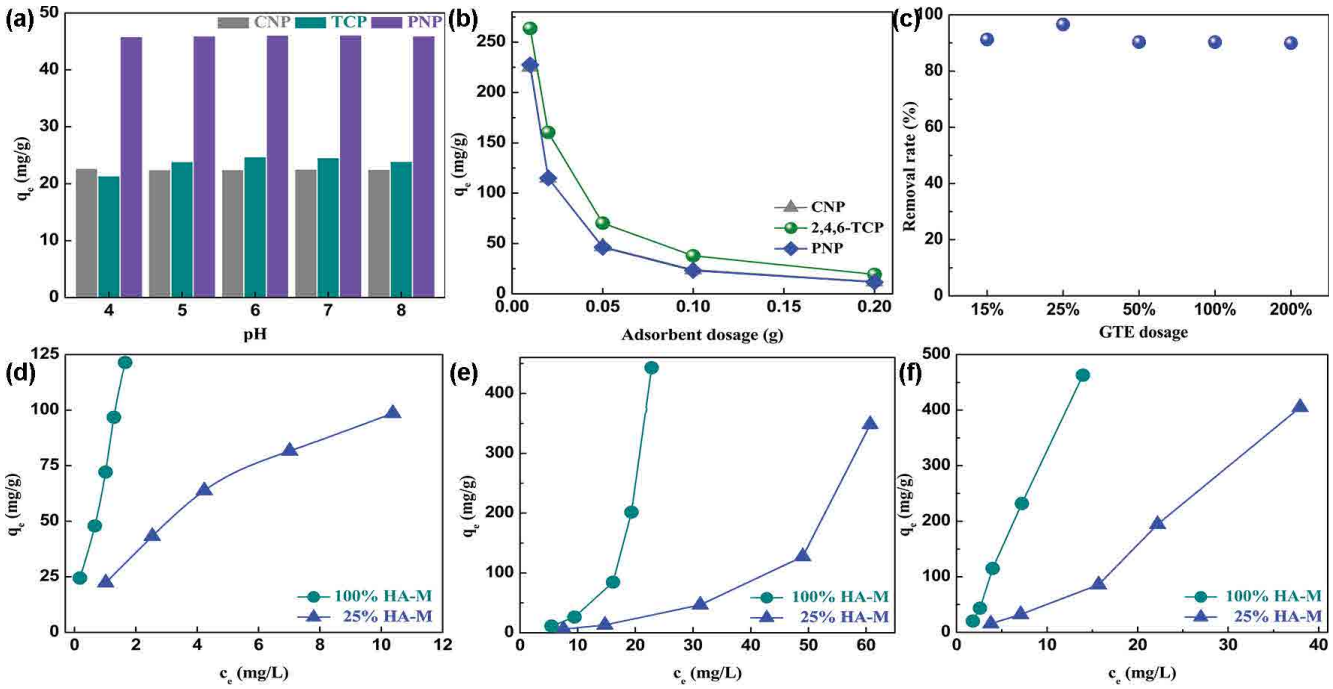

Fig. 3. Effect of factors on adsorption capacity in single-component system (a) pH, (b) adsorbent dosage; (c) effect of various GTE dosage on CNP removal rate; Effect of GTE dosage on COPs adsorption performance, (d) CNP, (e) 2,4,6-TCP and (f) PNP.

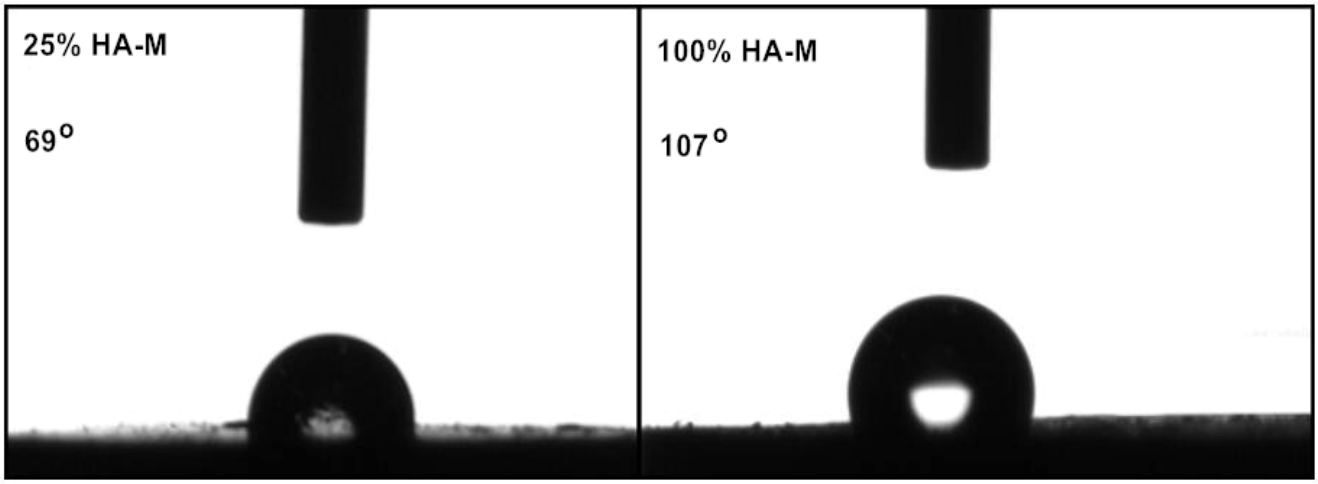

Fig. 4. Contact angles between water and the HAEE surface.

2,4,6-TCP and PNP, which generally correlate to the octanol–water partition coefficient of each COPs as well as the hydrophobic ability of HAEE [18,19].

3.3. Adsorption kinetic studies

As presented in Fig. 5, the adsorption capacity of HAEE to both TCP and PNP were higher than 100 mg/g in the initial 1.5 h of adsorption process, and the adsorption equilibrium for each COPs could be achieved within around 4 h (>60 mg/g for CNP, >110 mg/g for TCP and PNP). The fast adsorption rate could be attributed to the strong hydrophobic interactions between HAEE and COPs. Additionally, it was also believed that the mesoporous structure of adsorbent is beneficial for the reduction of mass transfer resistance [13,20].

As is shown in Fig. 6, it was obvious that the pseudo-second-order model could well describe the adsorption behaviors ($R^2 > 0.99$). The calculated equilibrium adsorption capacity of each COPs obtained from this model fitting was very close to the one determined by experiments (Table 1). For example, the calculated equilibrium adsorption capacity of PNP was about 122 mg/g while its experimental equilibrium adsorption capacity was almost 116 mg/g. Hence, it was not difficult to infer that "solid phase extraction" might

contribute to the dominated rate controlling step in the adsorption process.

3.4. Adsorption isotherm studies

Fig. 7 illustrates the experimental adsorption isotherms of HAEE to PNP, which was selected as a representative sample of COPs. When the concentration of PNP increased in the aqueous solution, the adsorption capacity of the modified adsorbent increased significantly at low concentrations, and then, shown a slow uptrend. It was also observed that the amount of PNP adsorbed increased slightly with a decrease in temperature, which signifies the exothermic nature of adsorption of COPs with HAEE. Therefore, the HAEE exhibited lower adsorption capacity at higher temperature.

Adsorption isotherms data were further fitted by Freundlich isothermal equation, which is expressed as:

$$q_e = K_3 C_e^{1/n} \tag{6}$$

where C_e is the equilibrium concentration (g/L), q_e is the equilibrium adsorption capacity (mg/g), K_3 is the Freundlich constant.

As shown in Fig. 7 and Table 2, the Freundlich model provided a good description to the isotherm data with correlation constant (R^2) higher than 0.97. The Freundlich model fitted the adsorption isotherms very well, and all the values of $1/n$ were small, which suggested that the adsorption of PNP on HAEE was easy to carry on. The Freundlich isotherm model meant that the adsorption process occurred on a heterogeneous surface of adsorbent [20,21]. The above experimental results suggest that the super adsorption capacities of HAEE should be ascribed to the introduction of the even distribution and strong hydrophobic properties of HAEE, which provide high affinity to the hydrophobic organic PNP.

In consideration of the fact that soil washing wastewater and/or ordinary polluted water often contain various

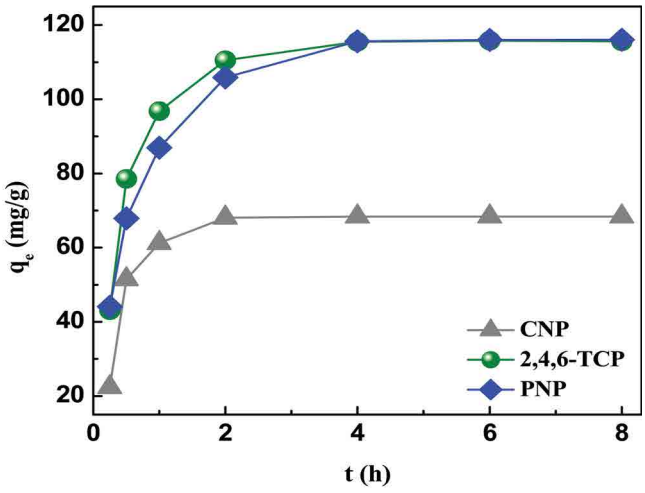

Fig. 5. Adsorption kinetics.

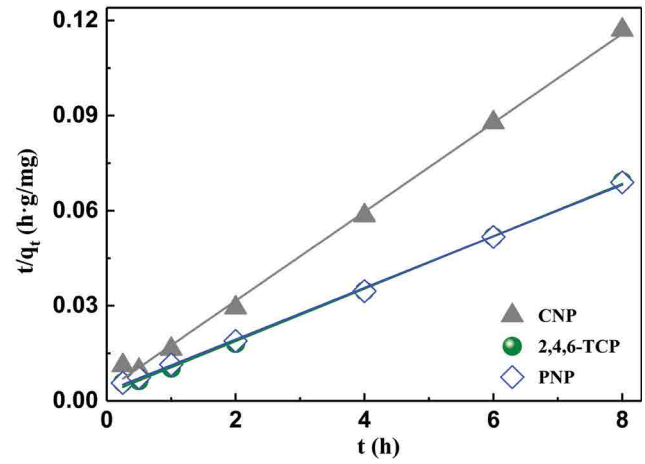

Fig. 6. Pseudo-second-order model fitting.

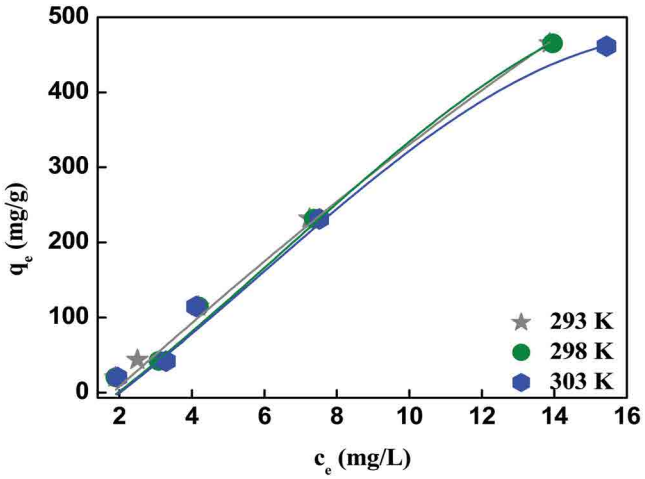

Fig. 7. Adsorption isotherm plots for adsorption of PNP onto HAEE.

Table 1
Fitting parameters collected from pseudo-second-order rate model

COPs	K_2 g/(mg h)	$q_{e,Cal.}$ mg/g	$q_{e,Exp.}$ mg/g	R^2	Error %
CNP	0.056	71.225	68.399	0.997	3.968
TCP	0.029	120.919	115.830	0.999	4.209
PNP	0.021	122.850	116.047	0.999	5.538

Er% = $[q_{e,Exp.} - q_{e,Cal.}]/q_{e,Cal.}$

Table 2
Freundlich model parameters

COPs		Freundlich		
		$1/n$	K_3	R_1^2
PNP	293 K	1.512	9.540	0.998
	298 K	1.540	9.658	0.986
	303 K	1.404	12.007	0.973

organic pollutants simultaneously, typical organic matters (benzene and phenol) were selected as the coexisting organics to investigate their influences on the adsorption of COPs on HAEE. The relevant result shows that these two coexisting organic matters have negligible influence on the adsorption performance of HAEE, indicating that the hydrophobicity performance of HAEE is dominant force during this process (Table 3).

3.5. Multi-component aqueous solutions

All kinds of COPs usually coexist in practical treatment wastewater (such as soil washing water) [22,23]. Thus, the adsorption performances of HAEE were investigated in aqueous solutions containing three typical COPs at different concentrations. As shown in Fig. 8, the adsorbent exhibited satisfied performances to all kinds of COPs both at low and high concentrations, including the adsorption capacities and the removal efficiency.

Comparing with the adsorption efficiency of HAEE to single COPs, the adsorption performances of HAEE toward these coexisting COPs were little worse, which shows that a mild competitive process existed among the is observed COPs. But, it is understood that the influence of the slight competitive effect can be negligible when it refers to the high removal efficiency. For instance, the removal efficiencies of PNP at different simulation groups (inset in Fig. 8c) at 8 h were >95%, ≈95%, >95%, respectively.

In addition, when compared with other adsorbents, the advantage of HAEE is the excellent adsorption ability to aromatic COPs with benzene rings through strong π-π interaction. The π-π bonding establishes between carbon-carbon double bonds or benzene rings of COPs molecules and benzene rings on the surface of HAEE via π-π coupling. Thus, it is not hard to expect that hydrophobic HAEE can provide a promising option for practical treatment of COPs-contained wastewater.

3.6. Regeneration of HAEE

In order to know the recyclability of HAEE, the adsorbent was reused for several times in adsorption of 2,4,6-TCP. As shown in Fig. 9, the HAEE could be recycled without significant loss of removal rate. The adsorption removal rate of 2,4,6-TCP was 95.82 % in the first cycle, while the adsorption removal rate of TCP declined to 83.83% in the third cycle. This relatively small change could be attributed to the strong "hydrophobic interactions" between HAEE and 2,4,6-TCP, which ensured a strong junction force during adsorption process. However, the recyclability of HAEE exhibited a slight decrease of removal in the following cycles, mainly due to the partial loss of HAEE during the regeneration process. Notably, the partial loss of the HAEE could be acceptable because of the environmentally friendly nature and ample of HA raw material.

Table 3
Effect of coexisting organic matters on the adsorption performance

COPs (removal efficiency)	Coexisting organic matters		
	Benzene	Phenol	Blank
2,4,6-TCP (%)	94.3[a]; 92.1[b]	92.2[a]; 90.7[b]	96.3

[a]Concentration of coexisting organic matters, 0.5 g/L.
[b]Concentration of coexisting organic matters, 1.0 g/L.

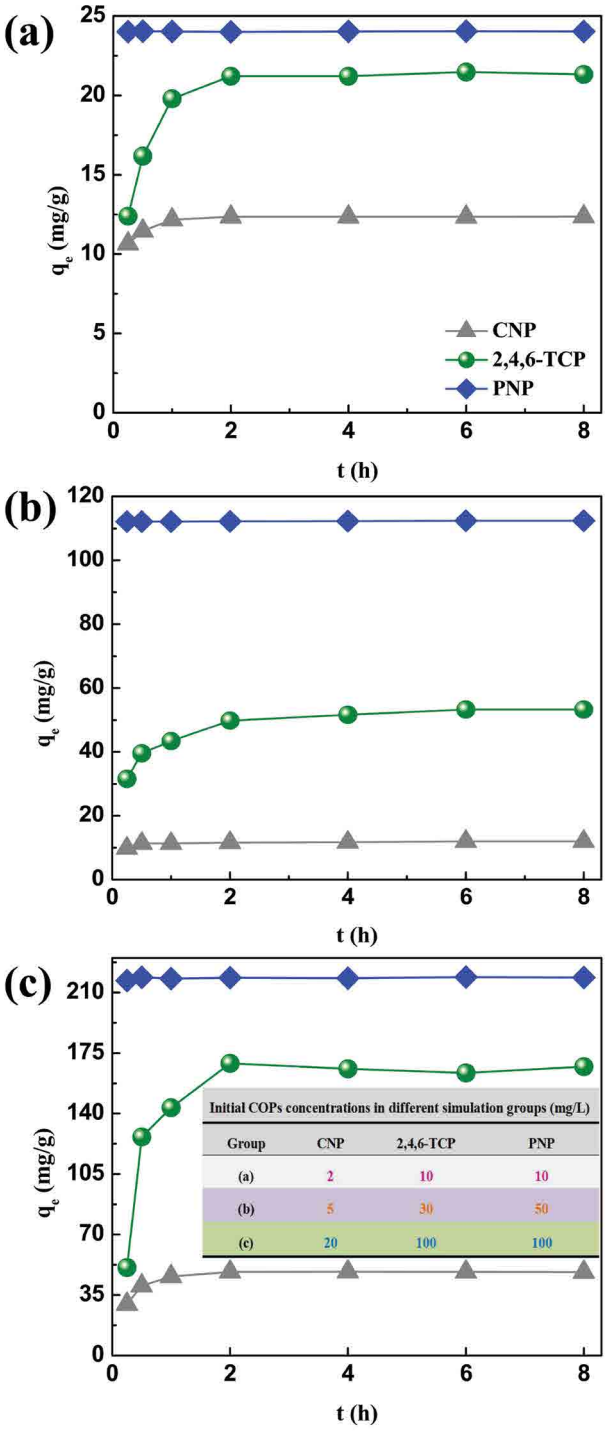

Fig. 8. Adsorption kinetics in multi-component aqueous solutions of various concentrations of COPs.

3.7. Innocuous treatment of COPs

Although, the adsorbed CNPs pollutants still have potential threat toward adjacent water, soil and gas environment due to persistent nature. As an interesting environmental material, TiO_2 has been widely used for organic pollutants treatment due to its good properties, such as cost effectiveness, strong oxidizing power and long-term stability against photo- and chemical corrosion [24]. Therefore, an efficient titanium dioxide-based photo-catalyst (Fe^0/F-TiO_2) was further synthesized and unitized to degrade the organic contaminant which was collected from desorption process, which is aimed to achieve the security treatment of COPs (Fig. 10). To further modify the band gap of TiO_2 by doping to extend the optical absorption properties into the visible light, here, fluorine (F) was introduced to the preparation process of photo-catalyst. In most cases, however, that mono-doping alone could not completely improve photo-catalytic activity. This was particularly because of the impurity band, which was partially occupied that, might act as recombination center and thus reduced the photogenerated current [25,26]. Hence, the Fe^0 was also introduced in the photo-catalytic material for providing the condition to form Fe^{2+}/Fe^0 interchange potential.

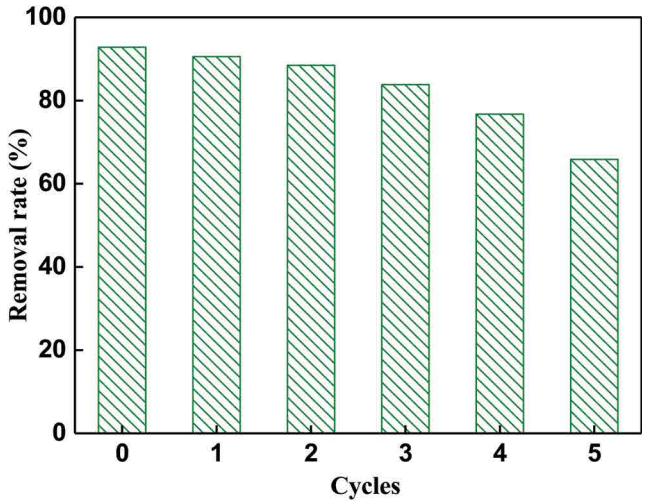

Fig. 9. Adsorption–desorption cycles of TCP onto HAEE.

As shown in Fig. 10, the crystalline phase, UV–Vis spectral data of Fe^0/F-TiO_2 catalyst were analyzed. Furthermore, the catalytic kinetics, the mineralization degree of 2,4,6-TCP and the possible photocatalytic degradation mechanism was explained. Under the visible light, the complete mineralization as well as the removal efficiency was observed within 12 h. A similar remarkable performance could be found for the dechlorination, where the extent of dechlorination was higher than 90% after 2 h of treatment. It was a clear indication that the Fe^0/F-TiO_2 was proved to be effective for the further degradation of COPs.

The possible photocatalytic degradation mechanism of 2,4,6-TCP was illustrated in Fig. 10d. With a conduction band and a valence band by visible light irradiation, the electron potential of TiO_2 provided the electrons to reduce Fe^{2+} to Fe^0, which may avoid the formation of oxide layer on the zero-value iron surface. The degradation process included three stages [27–31]: (i) Fenton-like photocatalytic oxidation dechlorination and ring opening; (ii) Fenton-like photocatalytic oxidation mineralization and further dechlorination; (iii) Fenton-like photocatalytic oxidation mineralization. First, photogenerated electrons (e^-) initiated from valence

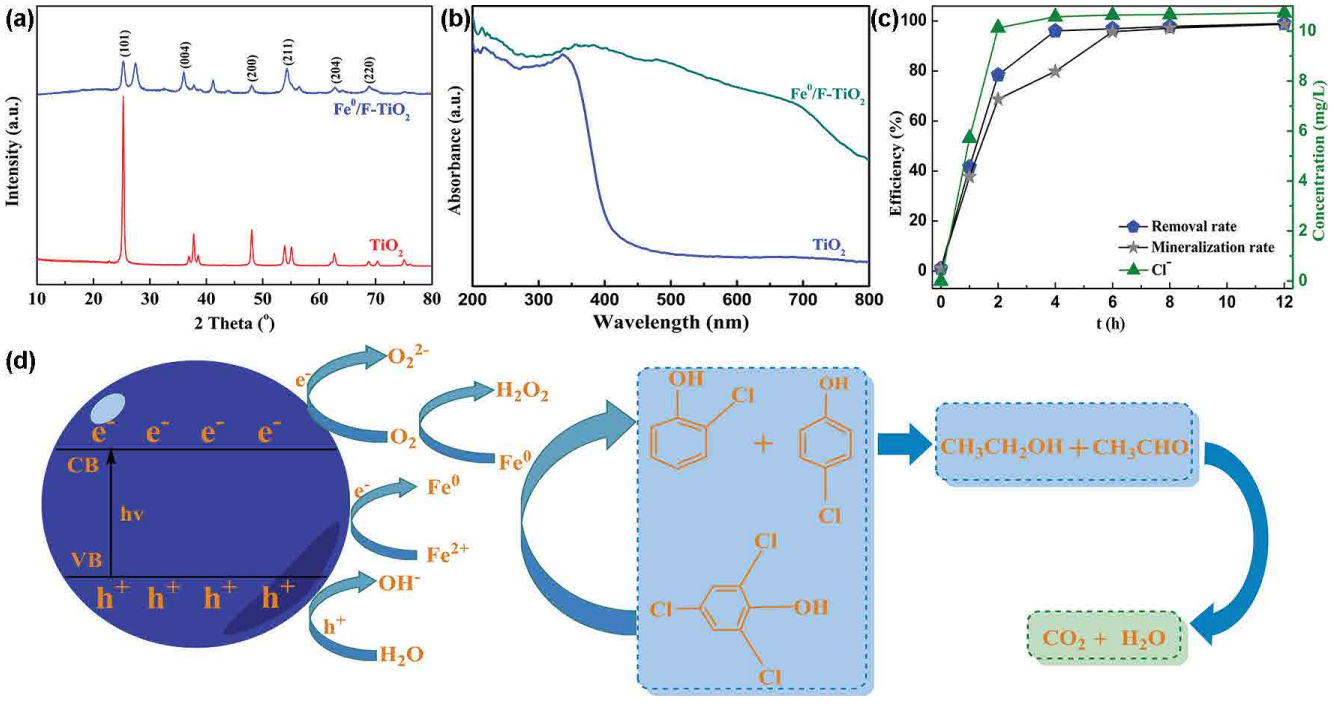

Fig. 10. (a) XRD pattern of photocatalyst, (b) UV–Vis spectral data of photocatalyst, (c) photocatalytic desorption of 2,4,6-TCP, and (d) the possible photocatalytic degradation pathway of 2,4,6-TCP.

band layer to conduction band layer and the holes (h^+) were generated at conduction band, when Fe^0/F-TiO_2 was exposed to electron radiation energy greater than its forbidden bandwidth. Then, O_2 and H_2O adsorbed on the Fe^0/F-TiO_2 surface would form highly active oxidized substances, including superoxide radicals ($^{\bullet}O_2$) and hydroxyl radicals ($^{\bullet}OH$), which may attack on the adjacent –Cl of 2,4,6-TCP. Sorts of dechlorination intermediates were formed by oxidation of 2,4,6-TCP, such as p-chlorophenol and 2-chlorophenol. Meanwhile, the environmental O_2 was unitized to produce H_2O_2, which was conducive to further open the benzene ring of intermediates. According to Fig. 10c, the dechlorination rate was about 90% while the mineralization rate was 70% within 2 h, and the dechlorination rate reached up to 100% when the mineralization rate was 80% in 4 h. It was clear to indicate that the dechlorination process occur synchronously with mineralization during the reaction. Finally, the small molecular organic compounds formed by oxidation ring opening were further mineralized by decarboxylation to CO_2 and H_2O.

4. Conclusions

The hydrophobic adsorbent (HAEE) exhibits noticeable efficiency in adsorptive removal of both mixed COPs and single component (CNP, 2,4,6-TCP or PNP) in aqueous solution. The adsorption studies showed that CNP sorption on HAEE reached high removal rate (>90%), whereas CNP sorption on HA was less than 50%. The adsorption kinetics demonstrated that the adsorption of COPs on HAEE reached equilibrium within 4 hours. The kinetic data were fitted well with the pseudo-second-order model. Additionally, HAEE can be recycled for several times without significant lose in its adsorption capacity. The hydrophobic interaction established between HAEE and COPs would be the dominated contributor in adsorption removal process. Moreover, the complete degradation of 2,4,6-TCP was achieved under visible light in the presence of Fe^0/F-TiO_2 catalyst. These results provide practical evidences about a promising potential idea of COPs treatment from wastewater and soil.

Acknowledgments

This work was supported by the National Natural Science Foundation of China (grant number 51641209).

References

[1] K. Kruanak, C. Jarusutthirak, Degradation of 2,4,6-trichlorophenol in synthetic wastewater by catalytic ozonation using alumina supported nickel oxides, J. Environ. Chem. Eng., 7 (2019) 102825.
[2] S. Benjakul, F. Bauer, Biochemical and physicochemical changes in catfish (*Silurus glanis* Linne) muscle as influenced by different freeze-thaw cycles, Food Chem., 72 (2001) 207–217.
[3] H. Kojima, M. Iida, E. Katsura, A. Kanetoshi, Y. Hori, K. Kobayashi, Effects of a diphenyl ether-type herbicide, chlornitrofen, and its amino derivative on androgen and estrogen receptor activities, Environ. Health Perspect., 111 (2002) 497–502.
[4] J. Kobayashi, M. Sakai, H. Kajihara, Y. Takahash, Temporal trends and sources of PCDD/Fs, pentachlorophenol and chlornitrofen in paddy field soils along the Yoneshiro River basin, Japan, Environ. Pollut., 156 (2008) 1233–1242.
[5] G.R. Chang, H.S. Chen, F.Y. Lin, Analysis of banned veterinary drugs and herbicide residues in shellfish by liquid chromatography-tandem mass spectrometry (LC/MS/MS) and gas chromatography-tandem mass spectrometry (GC/MS/MS), Mar. Pollut. Bull., 113 (2016) 579–584.
[6] L. Li, P.A.Q. Quinlivan, D.R.U. Knapp, Effects of activated carbon surface chemistry and pore structure on the adsorption of organic contaminants from aqueous solution, Carbon, 40 (2002) 2085–2100.
[7] W. Cai, J. Yu, M. Jaroniec, Template-free synthesis of hierarchical spindle-like γ-Al_2O_3 materials and their adsorption affinity towards organic and inorganic pollutants in water, J. Mater. Chem., 20 (2010) 4587–4594.
[8] X. Yang, C. Chen, J. Li, G. Zhao, X. Ren, X. Wang, Graphene oxide-iron oxide and reduced graphene oxide-iron oxide hybrid materials for the removal of organic and inorganic pollutants, RSC Adv., 2 (2012) 8821–8826.
[9] Q. Wen, Z. Chen, J. Lian, Y. Feng, N. Ren, Removal of nitrobenzene from aqueous solution by a novel lipoid adsorption material (LAM), J. Hazard. Mater., 209 (2012) 226–232.
[10] J. Ru, H. Liu, J. Qu, A. Wang, R. Dai, Removal of dieldrin from aqueous solution by a novel triolein-embedded composite adsorbent, J. Hazard. Mater., 141 (2007) 61–69.
[11] M. Lu, Y. Zhang, Y. Zhou, Z. Su, B. Liu, G. Li, T. Jiang, Adsorption-desorption characteristics and mechanisms of Pb (II) on natural vanadium, titanium-bearing magnetite-humic acid magnetic adsorbent, Powder Technol., 344 (2019) 947–958.
[12] Y. Cui, J. Yu, M. Su, Z. Jia, T. Liu, G. Oinuma, T. Yamauchi, Humic acid removal by gas–liquid interface discharge plasma: performance, mechanism and comparison to ozonation, Environ. Sci. Water Res., 5 (2019) 152–160.
[13] Y. Shen, S. Zhao, Y. Li, Q. Liu, C. Ma, H. Mao, Y. Liao, J. Ma, A feasible approach to dispose of soil washing wastes: adsorptive removal of chlorobenzene compounds in aqueous solutions using humic acid modified with monoolein (HA-M), RSC Adv., 7 (2017) 9662–9668.
[14] M.Z. Afzal, R. Yue, X.F. Sun, C. Song, S.G. Wang, Enhanced removal of ciprofloxacin using humic acid modified hydrogel beads, J. Colloid Interface Sci., 543 (2019) 76–83.
[15] H. Wang, J. Zhu, Q.L. Fu, J. W. Xiong, C. Hong, H.Q. Hu, A. Violante, Adsorption of phosphate onto ferrihydrite and ferrihydrite-humic acid complexes, Pedosphere, 25 (2015) 405–414.
[16] E. Illés, E. Tombácz, The effect of humic acid adsorption on pH-dependent surface charging and aggregation of magnetite nanoparticles, J. Colloid Interface Sci., 295 (2006) 115–123.
[17] N. Thinakaran, P. Baskaralingam, M. Pulikesi, P. Panneerselvam, S. Sivanesan, Removal of Acid Violet 17 from aqueous solutions by adsorption onto activated carbon prepared from sunflower seed hull, J. Hazard. Mater., 151 (2008) 316–322.
[18] M. Nakamura, T. Suzuki, K.I. Amano, S. Yamada, Relation of sorption behavior of agricultural chemicals in solid-phase extraction with their n-octanol/water partition coefficients evaluated by high-performance liquid chromatography (HPLC), Anal. Chim. Acta, 2 (2001) 219–226.
[19] J.E. Riviere, J.D. Brooks, Predicting skin permeability from complex chemical mixtures, Toxicol. Appl. Pharm., 2 (2005) 99–110.
[20] E.K. Radwan, H.H.A. Ghafar, A.S. Moursy, C.H. Langford, A.H. Bedair, G. Achari, Preparation and characterization of humic acid-carbon hybrid materials as adsorbents for organic micropollutants, Environ. Sci. Pollut. Res., 22 (2015) 12035–12049.
[21] Y. Shen, R. Yang, Y. Liao, J. Ma, H. Mao, S. Zhao, Tannin modified aminated silica as effective absorbents for removal of light rare earth ions in aqueous solution, Desal. Wat. Treat., 39 (2016) 18529–18536.
[22] J.C. Cancilla, R. Aroca-Santos, K. Wierzchoś, J.S. Torrecilla, Hazardous aromatic VOC quantification through spectroscopic analysis and intelligent modeling to assess drinking water quality, Chemometr. Intell. Lab. Sys., 156 (2016) 102–107.
[23] Z. Zhang, Z. Jiang, W. Shangguan, Low-temperature catalysis for VOCs removal in technology and application: a state-of-the-art review, Catal. Today, 264 (2016) 270–278.

[24] H. Su, Q. Li, T. Tan, Double-functional characteristics of a surface molecular imprinted adsorbent with immobilization of nano-TiO_2, J. Chem. Technol. Biotechnol., 11 (2006) 1797–1802.
[25] A. Khalilzadeh, S. Fatemi, Modification of nano-TiO_2 by doping with nitrogen and fluorine and study acetaldehyde removal under visible light irradiation, Clean Technol. Environ. Policy, 3 (2014) 629–636.
[26] D. Liu, R. Tian, J. Wang, E. Nie, X. Piao, X. Li, Z. Sun, Photoelectrocatalytic degradation of methylene blue using F doped TiO_2 photoelectrode under visible light irradiation, Chemosphere, 185 (2017) 574–581.
[27] T. Umebayashi, T. Yamaki, H. Itoh, K. Asai, Analysis of electronic structures of 3d transition metal-doped TiO_2 based on band calculations, J. Phys. Chem. Solids, 63 (2002) 1909–1920.
[28] W.P. Hsieh, J.R. Pan, C. Huang, Y.C. Su, Y.J. Juang, Enhance the photocatalytic activity for the degradation of organic contaminants in water by incorporating TiO_2 with zero-valent iron, Sci. Total Environ., 3 (2010) 672–679.
[29] E. Petala, M. Baikousi, M.A. Karakassides, G. Zoppellaro, J. Filip, J. Tuček, K.C. Vasilopoulos, J. Pechoušek, R. Zbořil, Synthesis, physical properties and application of the zero-valent iron/titanium dioxide heterocomposite having high activity for the sustainable photocatalytic removal of hexavalent chromium in water, Phys. Chem. Chem. Phys., 15 (2016) 10637–10646.
[30] P. Oleszczuk, M. Kołtowski, Effect of co-application of nano-zero valent iron and biochar on the total and freely dissolved polycyclic aromatic hydrocarbons removal and toxicity of contaminated soils, Chemosphere, 168 (2017) 1467–1476.
[31] Y. Yang, Q. Jin, D. Mao, J. Qi, Y. Wei, R. Yu, A. Li, S. Li, H. Zhao, Y. Ma, L. Wang, W. Hu, D. Wang, Dually ordered porous TiO_2-rGO composites with controllable light absorption properties for efficient solar energy conversion, Adv. Mater., 29 (2017) 160475.